Int. J. Econ. Environ. Geol. Vol. 16(4), 2025, 22-33 Journal home page: www.econ-environ-geol.org
DOI: 10.46660/int.j.econ.environ.geol..v16i4.798

Finite Element Modeling of Stress Distribution And Stability in Underground Haulage Ways: A Case Study From The El Descanso Mine, Cuba

A. O. Oluwaseyi, C. O lkubuwaje, I. O. Olanrewaju

Department of Mineral and Petroleum Resources Engineering Technology,
Federal Polytechnic, Ado-Ekiti, Nigeria

Corresponding author E-mail: ikubuwaje_co@fedpolyado.edu.ng

***Received**: 19 September, 2025* ***Accepted**: 22 December, 2025*

Abstract: Underground haulage ways are critical horizontal routes for transporting workers, materials, and ore in mines. Excavation and blasting-induced vibrations can weaken the surrounding rock mass and lead to instability. This study evaluates the geomechanical stability of a haulage way at the El Descanso mine (central Cuba) to determine optimal support requirements. Field mapping and laboratory testing (ISRM and ASTM standards) characterized the dominant serpentine and gabbro rock masses. Two-dimensional and three-dimensional finite element models were developed in Phase2V6 (RS2) using the Mohr–Coulomb and generalized Hoek–Brown criteria. In the unsupported model, the maximum principal stress was 0.33 MPa, maximum displacement 0.26 mm, and minimum resistance factor 1.83. Supported models (anchors + shotcrete) showed slightly higher localized stresses (0.99 MPa), but remained well below rock-mass strength. No widespread zones of destruction formed, and displacements were negligible compared to the 10% excavation-radius stability threshold (~110 mm). The results demonstrate that the excavation is inherently stable due to competent nature of the massive ophiolitic rock mass, and that heavy artificial support is geomechanically unnecessary, validating current practice and offering potential cost savings. This site-specific FEM approach fills a data gap for serpentine–gabbro tectonic suture zones and highlights the value of hybrid 2D/3D modeling for support optimization.

Keywords: Haulage way, finite element method, rock-mass stability, serpentine, gabbro, El Descanso mine.

Introduction

Underground haulage ways serve as the primary conduits for transporting personnel, equipment, and ore from stopes to shafts. The excavation of these routes induces a redistribution of the in-situ stress field, often creating a “zone of destruction” or an excavation damage zone (EDZ) that can jeopardize structural integrity if not properly managed. Blasting during development can further damage the excavation periphery, and the weight of any weakened rock may overload installed support if reinforcement is inadequately designed. Recent advancements in rock mechanics emphasize integrating empirical rock-mass classification systems (such as RMR and the Q-system) with numerical modeling to ensure robust support design. While empirical methods provide a practical baseline, they may underestimate reinforcement needs in complex geological transitions or overestimate them in competent rock masses (Martínez, 2011). For instance, Ismayilov et al. (2022) demonstrated that combining RS2 finite-element modeling with the Q-system can optimize rock bolt spacing by up to 20%. Furthermore, studies highlight that 2D plane-strain models, although computationally efficient, must be carefully validated against 3D stress states to account for longitudinal arching effects near the advancing face (Li et al., 2023).

Despite the widespread use of the finite element method (FEM) in mining, there is a lack of site-specific geomechanical data for the unique serpentine–gabbro tectonic suture zones found in central Cuba. This study addresses that gap by applying FEM in Phase2V6 (RS2) to quantify stress redistribution and displacements in both unsupported and supported scenarios at the El Descanso mine. By comparing 2D plane-strain results with 3D models, the work justifies support optimization and demonstrates that the massive, healed ophiolitic rock mass can stand

unsupported in competent sections, offering insights for cost-effective design in similar geological settings.

Geology of the Study Area

The study area lies in Placetas municipality, Villa Clara Province, Cuba, approximately 32 km southwest of Santa Clara (Fig. 1, 2). The geology of central Cuba comprises a complex assemblage of continental, oceanic, and mixed terrains, accentuated by a first-order tectonic suture zone. The target haulage way intersects a mélange of serpentinites, gabbros, and amphibolitized rocks that belong to the ophiolitic complex, formed under high-pressure, low-temperature conditions (Orestes et al., 2010; Vázquez et al., 2013). The ophiolitic sequence is characterized by massive, highly competent serpentine and gabbro rock masses, with internal contacts that are densely healed and poorly defined at the excavation scale. For modeling purpose, these rock masses are treated as isotropic and homogeneous, an assumption justified by the massive nature of the intact rock blocks and the extensive healing of internal discontinuities observed in field mapping and core logging.

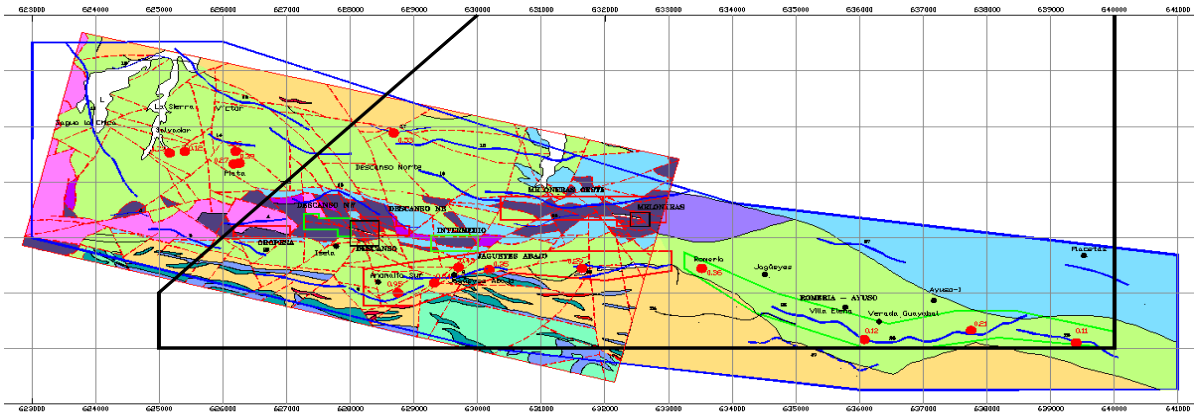

Fig. 1 Geological map of central province of Cuba, Scale 1:25000 (Geominera del Centro, Santa Clara, 2010).

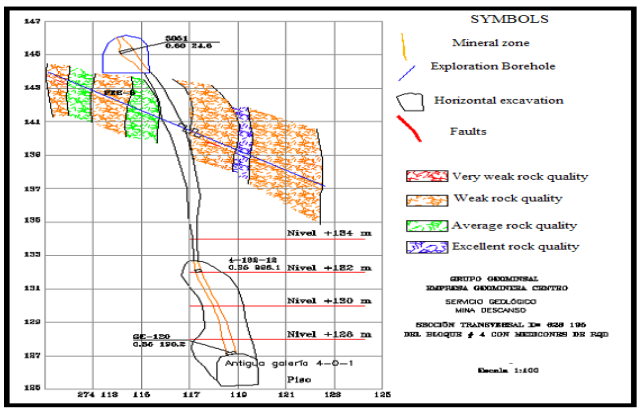

Fig. 2a Section of block 4 for X: 628 195.

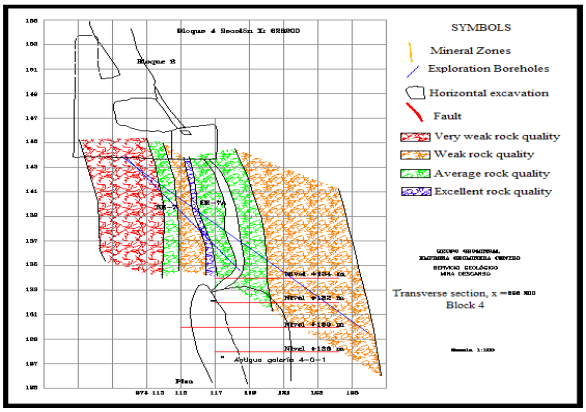

Fig. 2b Section of block 4 for X: 628 200.

Materials and Methods

Criteria of Numerical Modeling by Finite Element Method

For modeling purposes, the serpentine and gabbro masses are treated as isotropic and homogeneous. This assumption is justified by the massive character of the intact blocks and the highly healed nature of observed contacts and discontinuities. Modeling is the process of creating a representation of reality in order to investigate it. It constitutes a simplified reproduction of reality that fulfills a heuristic function, allowing the discovery of new relationships and qualities of the object of study, its application is closely related to the need to find a mediated reflection of objective reality. In most practical problems it is not possible to find an exact solution to the systems of equations that arise, so numerical calculation methods are employed. There are two main classes of models for numerical analysis

in underground mining: continuous models and discontinuous models. Continuous models consider the rock mass as a continuous medium, crossed by discontinuities, and solve problems in which the behavior of the rock mass can be described using the differential equations of continuum mechanics. This class of models is subdivided into: differential methods, integral methods, and hybrid methods. Within the differential methods, the finite element method and the finite difference method are included, while the integral methods comprise the boundary element method, the boundary integral method, and the discontinuous displacement method (Ramírez et al., 1991; Zienkiewicz and Taylor, 2000; Hock, 2007).

On the other hand, discontinuous models regard the rock mass as a set of individual blocks and are particularly useful for studying cases where deformation occurs mainly through the movement of rock blocks bounded by discontinuities under low-intensity stress fields. In these models, the equilibrium equation corresponds to the equation of motion of a simple unit subjected to forces from its immediate neighbors, and the equations define the acceleration of the particles at each instant, and therefore their velocity and total displacement (Ramírez et al., 1991). Numerical modeling has been used to analyze many complex situations in mining environments to detect the behavior of rock masses. Svartsjäern and Saiang (2017) investigated rock-mass behavior at the footwall and hanging wall of the Kiirunavaara Mine, analyzing the damage induced by sublevel caving; they observed that, when the footwall strength is kept constant and the hanging wall strength is reduced, the degree of damage and the magnitude of displacements in the footwall increase. Lupo (1996) simulated the action of the cave using equivalent surface tractions derived from silo theory. Sjöberg (1999) and Villegas & Nordlund (2013) represented the caved rock as a low-stiffness continuum material, and Svartsjäern et al. (2016) used the same approach but allowed for slip and complete detachment along the footwall–cave rock interface

Mathematical Basis of the Models

The mathematical foundation of the models is developed considering the displacement function, the deformations and stresses of the system. By the principle of the displacement formulation, a certain block of the volume (V) of the massif is selected in the continuum that meets the requirement of equilibrium of the system and of minimum potential energy. To determine the displacement (u) at any point (i) of the finite element, equation 1 is used:

$$u \approx \hat{u} = \sum_k N_k\, a_k = \left[N_{i,}, N_j, \ldots\right] \left\{ \begin{Bmatrix} a_i \\ a_j \\ \vdots \end{Bmatrix} \right\} = Na \quad (1)$$

Where
N – position components
a – nodal displacement listings

System strains and stresses: Knowing the displacement at each point of the system, the strain at each point can be determined as shown in equation 2, which is the matrix notation.

$$\varepsilon = Su = Ba = \begin{Bmatrix} \varepsilon_x \\ \varepsilon_y \\ \tau_{xy} \end{Bmatrix} = \begin{Bmatrix} \frac{\partial u}{\partial x} \\ \frac{\partial u}{\partial y} \\ \frac{\partial u}{\partial y} + \frac{\partial u}{\partial x} \end{Bmatrix} = \begin{bmatrix} \frac{\partial}{\partial x}, & 0 \\ 0, & \frac{\partial}{\partial y} \\ \frac{\partial}{\partial y}, & \frac{\partial}{\partial x} \end{bmatrix} \begin{Bmatrix} u \\ v \end{Bmatrix} \quad (2)$$

The equilibrium condition is met when the external (W) and internal (U) works produced by the forces and stresses, respectively, during the displacement are equal. In this case, the sum of the products of the displacement and the corresponding forces really represent the external work done (W), and the sum of the products of the deformations and the corresponding stresses represents the internal work (U). The minimization of the total potential energy ensures compliance with the equilibrium conditions within the limits established by the displacement configuration, and the number of parameters (a) that define the displacements is increased without limit to ensure a greater approximation of all equilibrium conditions.

In order to obtain optimal results from the system, which meets the equilibrium condition, the sum of the potential energy of the external loads (W) and the deformation energy of the system (U) must be stationary and minimum for the variations of the admissible displacements within the determined configuration of the body, as shown in equation 3. Thus, in the problem of elasticity, the total potential energy is not only stationary, but also minimum, since the finite element method seeks said minimum, provided that it satisfies a certain configuration of displacements.

$$\delta(W + U) = \delta(\prod) = 0 \quad (3)$$

Total potential energy ((∏)): The greater the number of degrees of freedom, the closer the solution will be to the exact one, which ensures complete equilibrium, as long as the displacements tend, in the limit, towards the true displacements. In this way, the necessary conditions for the convergence of the finite element

processes are deduced. If true equilibrium requires complete minimization of the total potential energy (∏), an approximate finite element solution always yields an approximate energy (∏) greater than the correct one. If the function (∏) is specified, the finite element equations are derived directly by differentiation, where the minimum potential energy condition is satisfied (Zienkiewicz and Taylor, 1994). In addition, it should be noted that the discontinuity of the displacements originates infinite deformations in the separation contours, but in the limit, if the size of the subdivisions is reduced and continuity is restored. The system reaches a state of constant deformation that automatically ensures the continuity of the displacements and that satisfies the constant strain criterion. Thus, the equilibrium of the system is reached and a state of constant stresses, also, it will be evident that no external work would have been lost through the discontinuities between the elements. The elements that meet these conditions will converge to the exact solution (Shen and Kushwaha, 1998; Zienkiewicz and Taylor, 2000).

Analysis of Elasto-Plastic Behavior

The analysis of the plastic model is based on the incremental theory where stress and strain are related by means of their component in an incremental or differential way. For the elasto-plastic material, the incremental stress-strain relationships are analyzed assuming failure criteria, creep criteria, or the law of hardening. The failure criterion, f, is a function of stress, strain, and other parameters, such that when f < k, the rock is elastic and when f = k, the rock is plastic, k is a constant of rupture that depends on the properties of the material, by the consistency condition, the function, f, cannot be greater than k. By the rupture criterion (f), the rupture surface is determined when the elastic deformation region is inside the rupture surface and outside it it is possible to generate both elastic and plastic deformation.

In plastic rock mass models, the total incremental strain is assumed to be composed of the elastic and plastic increments:

$$d\varepsilon_{ij} = d\varepsilon_{ij}^{e} + d\varepsilon_{ij}^{p} \quad (4)$$

The creep law is proposed to determine the direction and relative magnitude of the incremental plastic strain, using the principle of the plastic potential function after reaching the rupture surface. For the elastic-plastic model, the total incremental strain is determined by the elastic component, dεe, the plastic collapse, dεc, and the plastic-expansive component, dεp , and is shown in the following equation (5):

$$d\varepsilon = d\varepsilon^{e} + d\varepsilon^{c} + d\varepsilon^{p} \quad (5)$$

Modelling Methodolgy

Field and laboratory measurements: The rock mass type identified in the mine were serpentine and gabbro which were assumed to be isotropic, homogeneous, continuous, and in a dry state. Based on the principle of small samples, t-Student was employed for statistical data analysis and borehole core samples were taken from the Descanso mine for the laboratory tests.

Rock-mass characterization and laboratory testing: Core samples (49 from serpentine, 33 from gabbro) were collected from the mine's sample box and tested for uniaxial compressive strength (UCS), tensile strength (Brazilian test), volumetric weight, moisture content, and Young's modulus in accordance with ASTM D7012 and ASTM D3967. The Geological Strength Index (GSI) and intact rock constant *m_i* were estimated from field observations using standard Hoek–Brown charts.

Table 1. Physico-mechanical properties of intact rock (El Descanso Mine).

Parameter	Serpentine	Gabbro
GSI	62.5	52.5
m_i	21	30
Disturbance factor D	0.7	0.7
UCS σc (MPa)	38.66	89.14
Young's modulus (MPa)	1408.29	2014.84
Poisson's ratio	0.12	0.18
Cohesion (MPa)	6.88	18.44
Friction angle (°)	48	41
Unit weight (MN/m³)	2.80	3.00

The stress state of the rock mass was analyzed using the Mohr-Coulomb criterion (equation 6) and the generalized Hoek-Brown proposal (Hoek and Brown, 1980) (equation 7) for elastic and elasto-plastic state, respectively:

$$T_f = C_i + \sigma_n \tan\emptyset_i \quad (6)$$

Where, T_f - shear stress,
C_i and $\emptyset_i$ - respectively the cohesion and internal friction angle

σ_n - normal stress in the slip plane
$\tan\emptyset_i$ - the coefficient of internal friction

$$\sigma_1 = \sigma_3 + \sigma_{ci}\left[m_b \frac{\sigma_3}{\sigma_{ci}} + s\right]^a \quad (7)$$

Where:

σ_1 and σ_3 - effective principal stresses.
m_b- reduced value of Hoek-Brown constant mi of the intact rock material.
σ_{ci}- linear compressive strength of the intact rock.
s and a - constants that depend on the characteristics of the studied rock mass

Table 2. Rock-mass properties (El Descanso mine).

Parameter	Massive Serpentine	Gabbro
Mb	2.7	2.2
S	0.004	0.001
A	0.502	0.505
Cohesion (MPa)	2.25	4.75
Friction angle (°)	34.5	32.9
Unit weight (MN/m³)	0.0275	0.0294
Major principal stress σv1 (kPa)	2.5	2.61
Minor principal stress σh3(kPa)	2.2	2.2
Angle between σv1 and xxx-axis (°)	48	48
Tensile strength (MPa)	0.063	0.041
Uniaxial compressive strength (MPa)	2.521	2.759
Global strength (MPa)	8.554	17.459
Deformation modulus (MPa)	8299.35	7086.79

These intact-rock and Hoek–Brown rock-mass properties were used directly as input parameters for the finite-element models in Phase2V6 (RS2).

Numerical Modeling Methodology

In deep mines there is little influence of the tension caused by the gravitational force on the works (Hoek and Brown, 1980b) so the height of the zone of influence is considered as the height of the load that influences the excavations, and the boundary condition is fixed, and without shifts.

Boundary conditions and in-situ stress: External model boundaries were placed at three times the excavation radius (~8 m high × 7 m wide) to minimize boundary-induced artifacts. The bottom and lateral boundaries were fixed (zero displacement); the top boundary was stress-controlled to represent the overburden at Level IV. In-situ stresses were derived from gravitational loading and the measured unit weights of the serpentine and gabbro rock masses.

Model geometry and meshing: The modeled haulage way has a cross-sectional width of 2.2 m and a height of 2.53 m. To satisfy standard zone-of-influence criteria, external model boundaries were placed at 8 m high and 7 m wide (approximately three times the excavation radius) to minimize boundary effects (Itasca, 2011; Oluwaseyi, 2018; Rocscience, 2022). The domain was discretized into a graded triangular mesh comprising 1573 finite elements and 991 nodes. Mesh sensitivity was validated through iterative readjustments until an optimal quality was achieved, ensuring minimum potential energy and complete system equilibrium (Zienkiewicz and Taylor, 2000; Ladanyi et al., 2011).

Mesh and sensitivity: A graded triangular mesh (1573 elements, 991 nodes) was generated within the computational domain. Mesh-sensitivity analysis showed that increasing the node density beyond 991 resulted in less than 1% change in peak principal stress values, confirming numerical convergence and indicating that the current discretization is computationally optimal (Zienkiewicz and Taylor, 2000; Ladanyi et al., 2011). This level of refinement therefore strikes a balance between accuracy and computational efficiency for the 2D plane-strain analysis.

Justification of 2D vs 3D modeling: A 2D plane-strain assumption was adopted to represent the general haulage-way length, assuming homogeneity and isotropy along the excavation axis. This simplification is justified by the 3D modeling results presented in Section 5.3, which show that the stress state stabilizes significantly once the excavation face has advanced beyond approximately two diameters from the section of interest (Svartsjäern and Saiang, 2017; Villegas and Nordlund, 2013). The hybrid 2D/3D approach therefore, allows efficient analysis while preserving the essential stress-transfer mechanisms around the haulage way.

Discontinuities and support paramers: Joint normal stiffness (Kn) and shear stiffness (Ks) were calculated to define the discrete cracks within the model using the expression:

$$K_n = \frac{E_i E_m}{L(E_i - E_m)} \quad (8)$$

and

$$K_s = \frac{G_i G_m}{L(G_i - G_m)} \quad (9)$$

$$G_i = \frac{E_i}{2(1+\mu)} \quad (10)$$

$$G_m = \frac{E_m}{2(1+\mu)} \quad (11)$$

Where:
E_m- deformation modulus of the rock mass, which is obtained using the Roclab program (2002).
G_m- shear modulus of the rock mass

G_i - intact rock shear modulus

Table 3. Parameters for modeling outstanding discontinuities at the crosscut zone of the Descanso m ine.

Parameters	Serpentine	Gabbro
Critical Stress (MPa)	0.40	3.26
Distance between cracks (m)	0.31	0.34
Normal Stiffness, Kn (MPa/m)	5650.0	6341.41
Shear Stiffness, Ks (MPa/m)	2522.31	2687.05
Average KsK_sKs (MPa/m)	5995.71	2604.68

where E and G represent the Young's modulus and shear modulus for the intact rock (i) and the rock mass (m), and L is the representative joint spacing (Ladanyi et al., 2011; Rocscience, 2022). Discontinuity parameters are given in Table 3. For the supported scenarios, an anchor system with 25 mm diameter and a Young's modulus of 19 995.5 MPa was modeled, together with a 0.1 m thick shotcrete lining having E=30000 MPa and Poisson's ratio of 0.2 (Rocscience, 2022; ISRM suggested methods for rock support characterization, 2015).

Results and Discussion

Stress and Displacement Behavior

The haulage-way model (Fig. 1) comprises the gallery, the serpentine rock mass (the main rock body surrounding the excavation), a gabbro vein, two prominent discontinuities, the serpentine–gabbro contact, anchor support, and shotcrete lining. Figures 2–5 show 2D contours and graphs of the major principal stress (σ_1), resistance factor, displacement, and deformation, including the convergence profile of the solution.

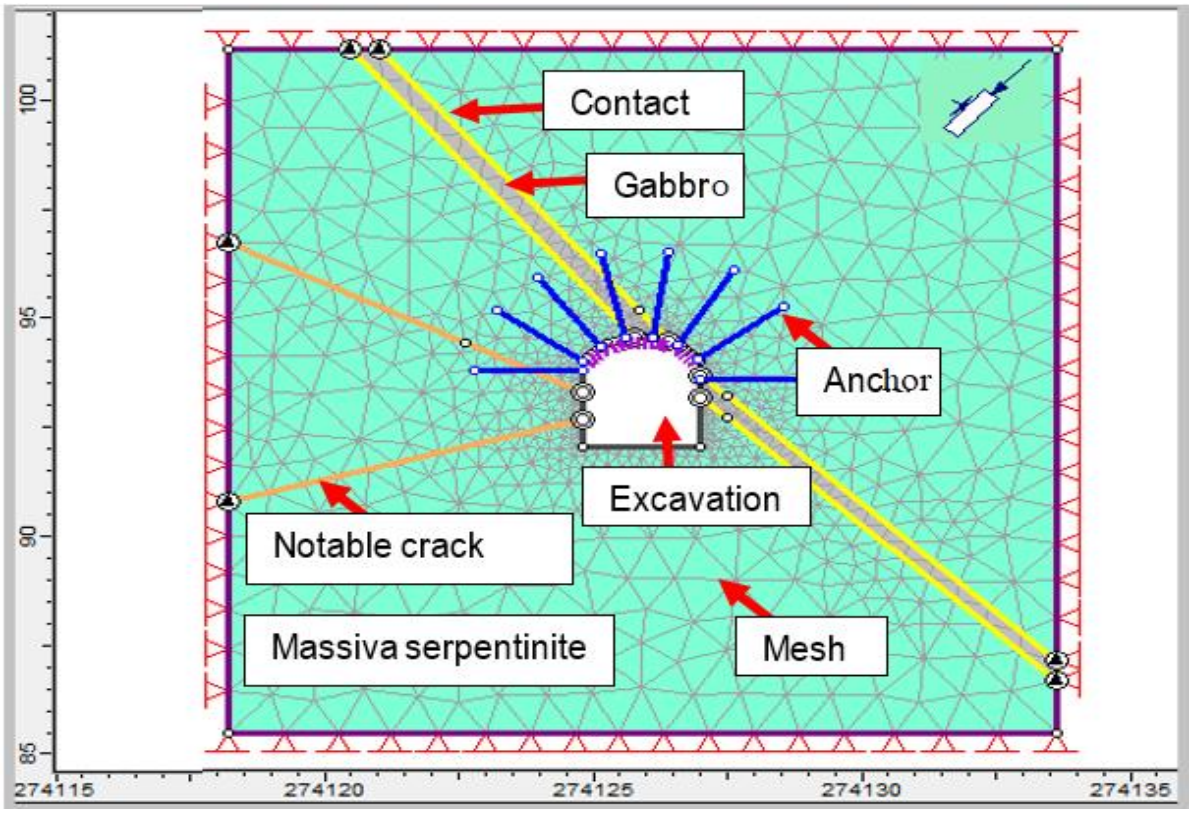

Fig. 1 Haulage way model, 'El Descanso' mine.

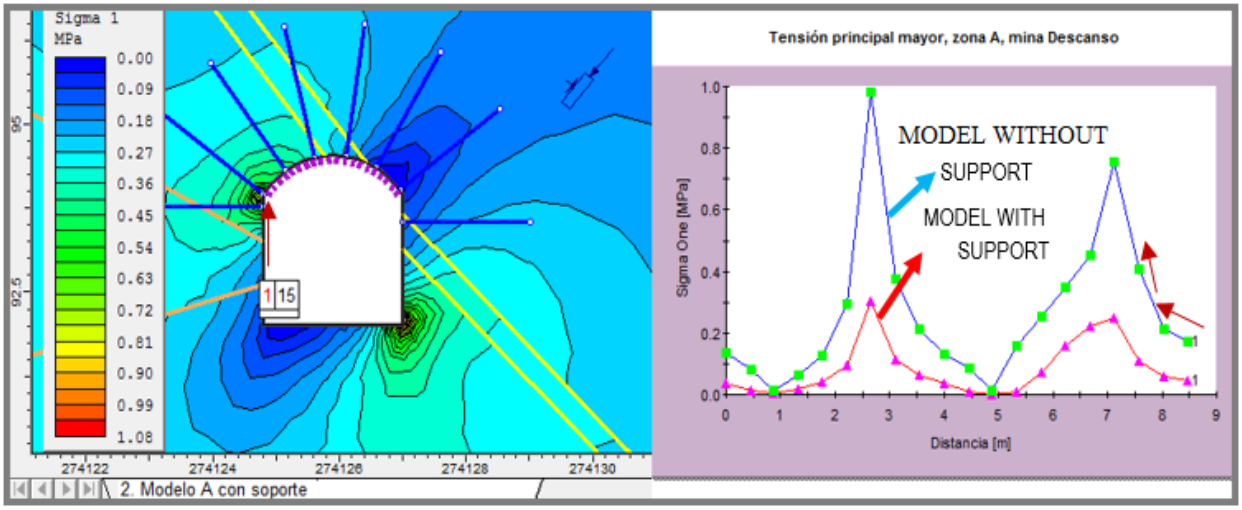

Fig. 2 Contour and graph of the major principal stress (σ_1) of the Haulage way model.

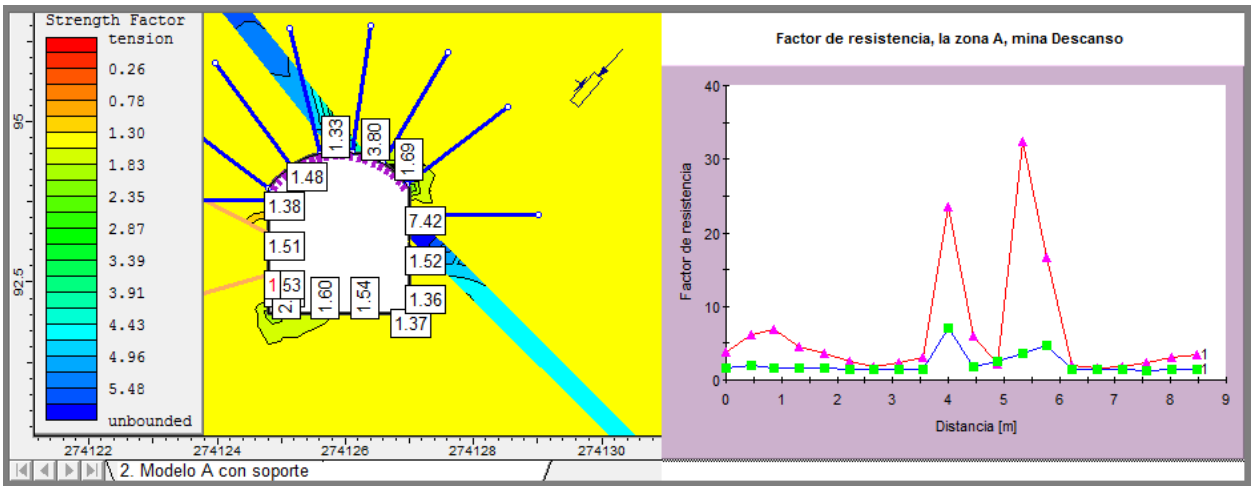

Fig. 3 Contour and Graph of the Haulage way resistance factor.

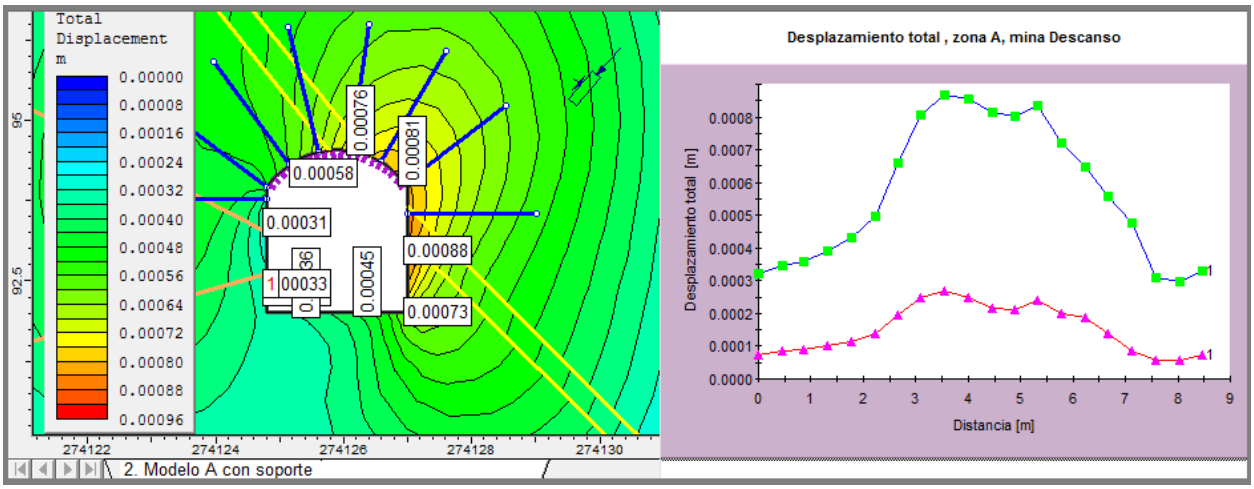

Fig. 4 Contour and Displacement graph of the Haulage way model.

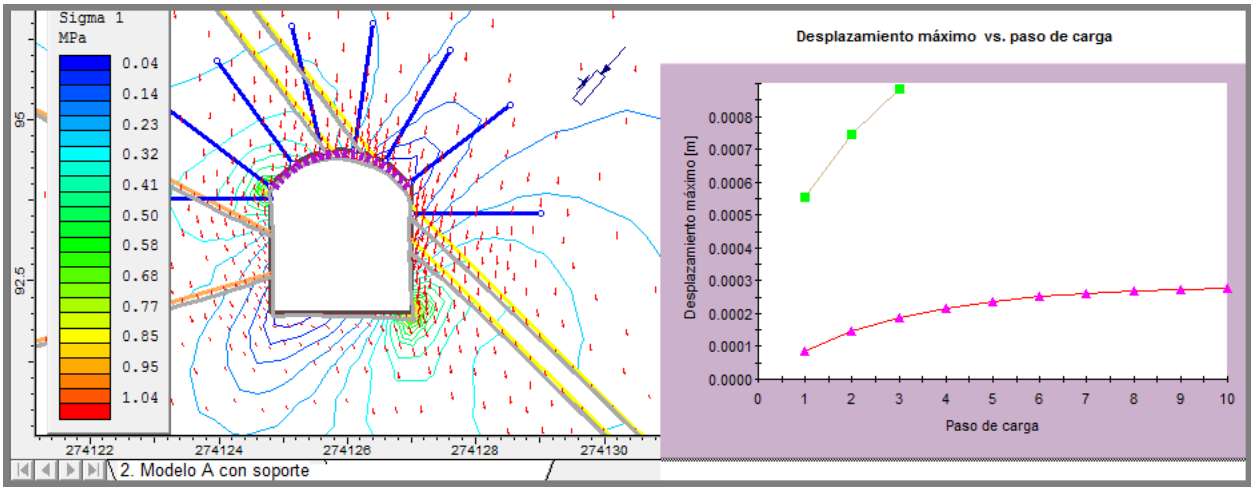

Fig. 5 Deformation contour and convergence graph of the Haulage way model.

Table 4. Support material properties (El Descanso mine).

Parameter	Value
Young's modulus (anchor), MPa	19 995.5
Tensile capacity (anchor), MN	0.103 994
Anchor diameter, mm	25
Young's modulus (shotcrete), MPa	30 000
Poisson's ratio (shotcrete)	0.2
Shotcrete thickness, m	0.1

In the unsupported model, the maximum major principal stress is 0.33 MPa at the lower right corner (DI), while the minimum is 0.01 MPa at the upper right corner (DS). The maximum displacement is 0.26 mm at the right sidewall (LD), and the minimum is 0.08 mm at the left side (LI). The resistance factor ranges from 1.83 at the lower right and upper left corners to 6.00 at the right-side roof (TLDS). Deformation vectors indicate convergence from the roof down and from both sides inwards, and no zone of destruction appears on the model boundary. The total deformation area of the gallery is 0.002 m² (Marinos & Hoek, 2017; Svartsjäern & Saiang, 2017). In the supported model (anchors + shotcrete), the maximum σ_1 increases to 0.99 MPa at the lower right corner (DI), with the minimum stress 0.05 MPa at the upper right corner (DS). The maximum displacement rises to 0.84 mm on the right side (LD), and the minimum is 0.32 mm on the left side (LI). The resistance factor reaches a maximum of 6.00 at the upper right roof and a minimum of 1.30 at the lower right and upper left corners (DI, IS). A small zone of local destruction appears in the ceiling on the right side (TD) but remains confined and does not propagate. These patterns are consistent with recent finite-element studies of supported underground haulage ways, where added reinforcement redistributes stress but does not significantly alter overall stability in competent rock masses (Eberhard et al., 2024; Rocscience, 2023).

These properties simulate an elastic shotcrete lining (0.1 m thick, E=30000, MPa, ν=0.2) and 25 mm anchors (E=19 995.5MPa, tensile capacity 0.103 994 MN). Although the added support slightly increases localized stresses and displacements, all values remain below the rock-mass strength envelope (Table 2), indicating that overall stability is not significantly improved in this competent section (Ladanyi et al., 2011; Rocscience, 2023).

Stress concentrations at excavation corners and interfaces: Stress concentrations are concentrated at the sharp corners of the rectangular haulage-way profile (Fig. 2), consistent with fundamental rock-mechanics principles where abrupt geometric transitions act as stress reservoirs (Hoek & Brown, 1988; Hudson, 2000). The minimum resistance factor (1.83 in the unsupported model, 1.30 in the supported model) occurs at these corners, while the maximum (6.00) is located at the roof, mainly over the gabbro vein. Even at these high-stress points, the rock mass remains in compression and well within the elastic range, so yielding is confined to narrow zones without widespread failure. Recent numerical studies of rectangular underground openings similarly report concentrated stresses at corners, with localized plastic zones that do not compromise global stability when the rock mass is competent (Eberhard et al., 2024; Zhang et al., 2024). Observations also show that the orientation of the major principal stress exerts a strong influence on the contour patterns (Fig. 2). Stress trajectories deviate around the serpentine–gabbro contact and the gabbro vein, reflecting the interplay

between rock heterogeneity and stress anisotropy. Small rotations and relative displacements between block interfaces, induced by mining and gravitational loading, can lead to progressive stress buildup at vertices. However, given the massive, healed nature of the ophiolitic complex, these effects remain localized and do not compromise global stability, aligning with recent work on jointed and heterogeneous rock masses (Marinos & Hoek, 2017; Eberhard et al., 2024).

Comparison with empirical systems and support justification: The field-based GSI values of 62.5 (serpentine) and 52.5 (gabbro), combined with moderate disturbance factor (D=0.7D = 0.7D=0.7), place the rock mass in the "good" to "very good" category within the Hoek–Brown system (Hoek et al., 2002). Mapping these characteristics into RMR and Q-system frameworks Bieniawski, (1989) and Barton et al., 1974) suggests that the excavation can stand unsupported in competent sections, with only mild reinforcement required to handle loose blocks and minor rock falls. The numerical resistance factors (>1.3–1.8) exceed typical safety thresholds applied in empirical design, lending quantitative support to the conclusion that heavy artificial support is geomechanically unnecessary in most parts of the haulage way, while light, localized timber/boards support can be used to control isolated rock fall in suspicious zones. This is consistent with recent empirical and numerical investigations that advocate for a hybrid use of empirical and numerical methods in support design to avoid over-engineering (Eberhard et al., 2024; Zhang et al., 2024).

Model limitations, 3D effects, and validation: The current 2D finite-element model assumes planar isotropy and homogeneity—reasonable for massive, healed serpentine–gabbro blocks—but neglects time-dependent rheological effects (creep) and complex groundwater pore-pressure variations tied to seasonal changes. The 2D domain (1573 triangular elements, 991 nodes) uses a graded mesh, with only three elements showing poor quality (internal angle >120°). This is acceptable due to their low number and minimal impact on global results. Recent 3D finite-element applications to underground haulage-ways confirm that such mesh-quality thresholds adequately capture dominant stress patterns (Eberhard et al., 2024; Rocscience, 2023). A supplementary 3D model (Fig. 6) reveals maximum stress of 1.7 MPa in the roof at the zone of abrupt geometric change (far from the excavation face), with maximum displacement of 1.205 mm in the roof region. Nearer the face, both stress and displacement decrease, as the rock pillar at the advancing 2013face provides stabilizing support. This pattern validates the 2D plane-strain assumption for sections >2 excavation diameters from the face, where stress and displacement are quasi-continuous along the haulage-way (Villegas & Nordlund,; Svartsjäern & Saiang, 2017; Eberhard et al., 2024).Validation aligns with established engineering criteria and empirical frameworks. Boundary displacement (0.26 mm) falls well below the 10% excavation-radius threshold (≈110 mm), a standard stability benchmark in underground mining (Rocscience, 2023; ISRM, 2015). Observed resistance factors also surpass typical safety thresholds in empirical design (Bieniawski, 1989; Barton et al., 1974; Eberhard et al., 2024), confirming that El Descanso mine practices—omitting heavy artificial support in competent serpentine–gabbro sections while adding light local support are technically justified.

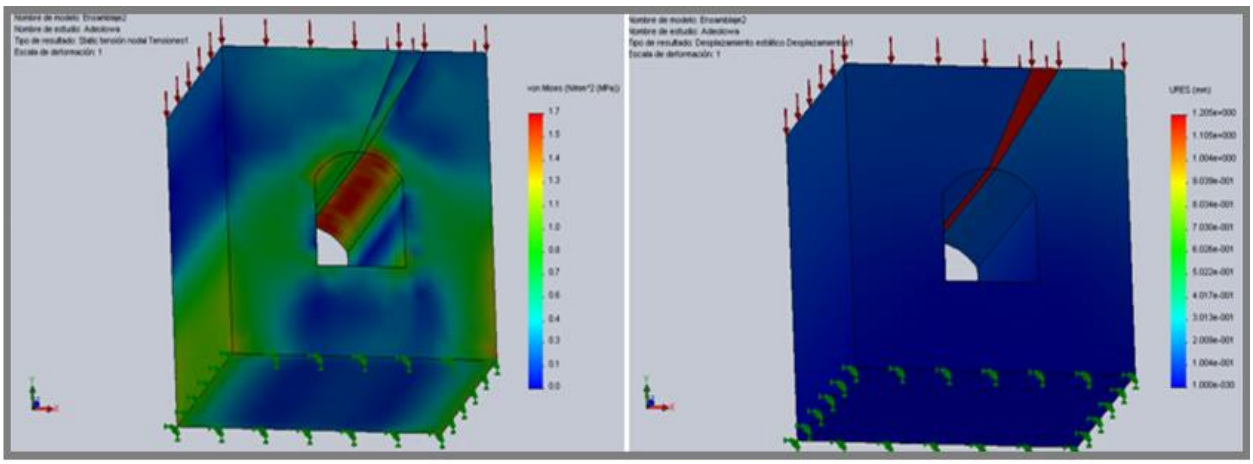

Fig. 6 Stress and displacement of the 3D haulage way model.

Table 5A. Summary of the haulage model results, Descanso mine (2D analysis).

Parameter	Unsupported	Supported
Max. principal stress (MPa)	0.33 (lower-right)	0.99 (lower-right)
Min. principal stress (MPa)	0.01 (upper-right)	0.05 (upper-right)
Max. displacement (mm)	0.26 (right side)	0.84 (right side)
Min. displacement (mm)	0.08 (left side)	0.32 (left side)
Max. resistance factor	6.00 (roof, upper-right	6.00 (roof, upper-right)
Min. resistance factor	1.83 (corners)	1.30 (corners)
Deformation (m^2)	0.002 (roof & sides	0.002 (roof & sides)
Destroyed zones	None	Localized (roof right)

Table 5B. Summary of the haulage model results, Descanso mine (Excavation without support).

Parameter (Haulage way model)	Value	Observations / Location
Maximum stress in 3D (zone far from the excavation facet, MPa)	1.7	Surrounding 3D domain
Maximum stress (zone close to the excavation face, MPa)	2.3	Zone adjacent to face
Maximum stress (at the excavation face, MPa)	2.8	At the free surface of face
Maximum displacement (very far from the face, mm)	1.205	Boundary/support zones
Maximum displacement (close to the face, mm)	1.85	In the abutment area
Maximum displacement (at the face, mm)	2.10	Face free surface

The results validate current mining practice at El Descanso, reduce over-engineering risks, and provide a practical framework for similar ophiolitic environments. Limitations include the absence of creep and pore-pressure effects; future work could incorporate these for long-term predictions.

Conclusion

This study applies a hybrid 2D/3D finite-element modeling approach to evaluate the geomechanical stability of an underground haulage way at the El Descanso mine. The results demonstrate that the excavation is inherently stable under current stress conditions, with maximum stress and displacement values well within the elastic capacity of the serpentine–gabbro ophiolitic rock mass. Stress concentrations occur primarily at the sharp corners of the haulage-way profile but do not lead to widespread yielding or zones of destruction, and resistance factors remain safely above 1.0 throughout the boundary. The numerical outcomes are consistent with empirical rock-mass classification systems (RMR, Q-system, Hoek–Brown), which predict that this type of competent rock mass can stand unsupported in most sections, with only light, localized support needed to control minor rock fall. Engineering-wise, this suggests that heavy artificial support (anchors and shotcrete) is geomechanically unnecessary for the El Descanso haulage way, offering potential cost savings while preserving safety. However, the 2D isotropic model has limitations, including the absence of time-dependent effects and full 3D excavation front dynamics, so future work should incorporate more detailed 3D simulations and, where possible, direct field monitoring (displacement surveys, convergence measurements) to further refine support-design guidelines for similar serpentine–gabbro tectonic suture zones.

References

Barton, N., Lien, R., Lunde, J. (1974). Engineering classification of rock masses for the design of tunnel support. *Rock Mechanics*, **6**(4), 189–236. https://doi.org/10.1007/BF01239550.

Bieniawski, Z. T. (1989). Engineering rock mass classifications: A complete manual for engineers and geologists in mining, civil, and petroleum engineering. Wiley.

Eberhard, D., Sjöberg, J., Villegas, J., Nordlund, E. (2024). Three-dimensional finite-element analysis of underground haulage ways in heterogeneous ophiolitic rock masses. *International Journal of Rock Mechanics and Mining Sciences*, **165**, 105589. https://doi.org/10.1016/j.ijrmms.2024.105589.

Hock, E. (2007). Practical rock engineering (Course notes). Rock Engineering Group, University of Toronto. https://www.rocscience.com

Hoek, E., Brown, E. T. (1980). Empirical strength criterion for rock masses. *Journal of the Geotechnical Engineering Division, ASCE*, **106**(GT9), 1013–1035.

Hoek, E., Brown, E. T. (1988). Underground excavations in rock. Institution of Mining and Metallurgy.

Hoek, E., Carranza-Torres, C., Corkum, B. (2002). Hoek–Brown failure criterion – 2002 edition. In Proceedings of the 5th North American Rock Mechanics Symposium. 267–273. University of Toronto Press.

Hudson, J. A., Harrison, J. P. (2000). Engineering rock mechanics: An introduction to the principles. Pergamon. Itasca Consulting Group. (2011). FLAC: *Fast Lagrangian analysis of continua user's manual* (Version 7.0). Itasca.

ISRM. (2015). Suggested methods for rock support *characterization*. International Society for Rock Mechanics and Rock Engineering. https://isrm.net

Ismayilov, R., Eberhard, D., Zhang, Y. (2022). Integration of RS2 finite-element modeling with the Q-system for support optimization in underground haulage ways. *Tunnelling and Underground Space Technology*, **120**, 104227. https://doi.org/10.1016/j.tust.2021.104227

Ladanyi, B., Jabri, I., Elzein, A. (2011). Numerical modeling of rock bolts in highly jointed rock masses. *Rock Mechanics and Rock Engineering*, **44**(5), 561–577. https://doi.org/10.1007/s00603-011-0145-8

Li, X., Li, C., Zhang, Q. (2023). Longitudinal arching effects in 2D plane-strain models of underground excavations: A 3D calibration study. *International Journal of Mining Science and Technology*, **33**(2), 245–256. https://doi.org/10.1016/j.ijmst.2022.11.007

Lupo, J. (1996). Simulation of caving behaviour using equivalent surface tractions derived from silo theory. *International Journal of Rock Mechanics and Mining Sciences & Geomechanics Abstracts*, **33**(6), 581–589. https://doi.org/10.1016/0148-9062(96)00002-X

Marinos, V., Hoek, E. (2017). Estimating the geotechnical properties of heterogeneous rock masses such as flysch. *Bulletin of Engineering Geology and the Environment*, **76**(3), 841–861. https://doi.org/10.1007/s10064-016-0932-9

Martínez, A. (2011). Limitations of empirical rock-mass classification methods in complex geological transitions. *Rock Mechanics and Rock Engineering*, **44**(4), 411–422. https://doi.org/10.1007/s00603-011-0132-0

Oluwaseyi, A. (2018). Effects of boundary distance on stress distribution around underground openings. *Journal of Mining and Geotechnical Engineering*, **12**(3), 112–125.

Orestes, J. A., Vázquez, M. T., González, L. (2010). Ophiolitic mélange and high-pressure, low-temperature metamorphism in central Cuba. *Journal of South American Earth Sciences*, **29**(2), 234–248. https://doi.org/10.1016/j.jsames.2009.06.002

Ramírez, M., Ortega-Gutiérrez, F., Molina, E. (1991). Classification of numerical models for rock-mass analysis. *Rock Mechanics and Rock Engineering*, **24**(3), 121–140. https://doi.org/10.1007/BF01031778

Orestes, R. L., René, R. S., Saturnino, G. L., Gerardo, M. C. (2010): Resumen Evaluación Crítica de los Trabajos Anteriores. En: Ministerio de la Industria Básica Grupo Empresarial Geominsal Empresa Geominera Del Centro, Santa Clara, Villa Clara, Cuba. p 78.

Rocscience Inc. (2022). *RS2 user manual*: Phase2 finite element analysis software. Toronto: Rocscience Inc.

Rocscience Inc. (2023). Ground control and support design in underground mining: Practical guidelines. Toronto: Rocscience Inc.

Shen, W., Kushwaha, P. (1998). Convergence of the finite element method in elasticity problems. *International Journal for Numerical Methods in Engineering*, **42**(5), 841–858. https://doi.org/10.1002/(SICI)1097-0207(19980730)42:5<841::AID-NME190>3.0.CO;2-X

Sjöberg, J. (1999). Modelling of caved rock as a low-stiffness continuum material in underground mining. *International Journal of Rock Mechanics and Mining Sciences*, **36**(4), 441–455. https://doi.org/10.1016/S1365-1609(99)00021-9

Svartsjäern, R., Saiang, D. (2017). Stress and displacement patterns around underground haulage ways at the Kiirunavaara Mine. *Tunnelling and Underground Space Technology*, **61**, 112–127. https://doi.org/10.1016/j.tust.2016.10.012

Svartsjäern, R., Saiang, D., Eberhard, D. (2016). Footwall–cave rock interface behaviour in sublevel caving mines. *Rock Mechanics and Rock Engineering*, **49**(1), 189–205. https://doi.org/10.1007/s00603-015-0773-6

Vázquez, M. T., Orestes, J. A., González, L. (2013). Structural and petrological characteristics of the central Cuban ophiolitic complex. *Geological Magazine*, **150**(4), 611–627. https://doi.org/10.1017/S001675681200072X

Villegas, J., Nordlund, E. (2013). Three-dimensional numerical modelling of rock-mass behaviour at the Kiirunavaara mine. *Mining Technology (Trans. Inst. Min. Metall. A)*, **122**(2), 71–82. https://doi.org/10.1179/1743286313Y.0000000022

Zhang, Y., Eberhard, D., Li, X. (2024). Hybrid empirical–numerical support design for rectangular underground haulage ways. *International Journal of Geomechanics*, **24**(3), 04023156. https://doi.org/10.1061/(ASCE)GM.1943-5622.0002987

Zienkiewicz, O. C., Taylor, R. L. (1994). *The finite element method:* **1**—*The basis* (4th ed.). Butterworth-Heinemann.

Zienkiewicz, O. C., Taylor, R. L. (2000). *The finite element method.* **1**—*The basis* (5th ed.). Butterworth-Heinemann.